Hindawi
Journal of Food Quality
Volume 2023, Article ID 2301485, 11 pages
https://doi.org/10.1155/2023/2301485

Research Article

Characterization of Arrowhead-Derived Type 3 Resistant Starch Prepared by Ultrasound-Assisted α-Amylase Degradation

Jian Sun,[1] Liangge Sun,[2] Xinxiang Chen,[2] Husnain Raza,[3] Gangshan Wu ,[1] Qiufang Liang,[2] and Xiaofeng Ren [2,4]

[1]*School of Information Engineering, Jiangsu Vocational College of Agriculture and Forestry, Jurong 212400, China*
[2]*School of Food and Biological Engineering, Jiangsu University, 301 Xuefu Road, Zhenjiang, Jiangsu 212013, China*
[3]*Institute for Advanced Study (IAS), Shenzhen University, No. 3688, Nanhai Avenue, Nanshan District, Shenzhen, Guangdong 518060, China*
[4]*Jiangsu Provincial Key Laboratory for Physical Processing of Agricultural Products, Zhenjiang, Jiangsu 212013, China*

Correspondence should be addressed to Gangshan Wu; wugangshan@jsafc.edu.cn and Xiaofeng Ren; renxiaofeng@ujs.edu.cn

Received 24 October 2022; Revised 26 November 2022; Accepted 2 December 2022; Published 3 January 2023

Academic Editor: Vita Di Stefano

The effect of ultrasonic-assisted α-amylase hydrolysis on the structure and physicochemical properties of arrowhead-derived type 3 resistant starch (RS3) was studied. After ultrasound treatment, the yield of resistant starch reached 17.21%, significantly ($p < 0.05$) increased by 65.64%. Compared with RS3 prepared by traditional enzymolysis (RS3-E), the crystal form and chemical bond of RS3 prepared by ultrasonic-assisted enzymolysis (RS3-UAE) did not change, but its gelatinization temperature, relative crystallinity, enthalpy, and 1047/1022 values were improved to varying degrees. RS3-UAE exhibited a higher solubility, transparency, water absorption capacity, and higher swelling power at 70°C. The analysis results of iodine absorption, differential scanning calorimetry, X-ray diffraction, Fourier transform-infrared spectroscopy, and scanning electron microscopy demonstrated that RS3-UAE exhibited a more regular shape, smoother surface, higher crystallinity, stable double helix structure, and more ordered and denser structure. Therefore, ultrasound-assisted enzymatic technology is an effective way to prepare RS3, and it can improve the functional and structural properties of the prepared RS3 to a certain extent.

1. Introduction

A well-known dietary fiber, resistant starch (RS), is a combination of starch and starch indigestible degradation products in the human small intestine [1, 2]. Having desirable physicochemical characteristics such as mild taste, white appearance, increased viscosity, swelling, water binding capacity, and gel formation, RS can be used as food additives [3]. Furthermore, RS is widely used as a functional food due to its potential health benefits, such as controlling obesity and diabetes, reducing the risk of cardiovascular disease, and colon cancer. [4] RS can be divided into four types, namely, RS1-RS4, among which RS3 has good thermal stability and has proven safe and healthy [5]. For the last few years, the food science community has been paying much more attention to the research and application of RS3 in the food industry.

In the formation of RS3, some short-chain starch escapes into the solution from fully hydrated starch granules as a random coil polymer, and then it begins to reassociate at low temperatures, forming a stable double helix structure through hydrogen bonding [6]. The RS3 yield is affected by the botanical source of the starch, the amylose/amylopectin ratio, the degree of gelatinization, processing, and storage conditions [7]. In general, amylose is more appropriate for recrystallization than highly branched amylopectin, favoring the formation of RS3. Furthermore, numerous studies also reported physicochemical properties of amylose directly influence the RS3 formation, including amylose chain length, amylose content, and amylose retrogradation [8, 9]. At present, enzyme treatment has been proven to be a green, inexpensive, and efficient way of debranching the amylopectin and formation of amylose [6]. However, starch

granules have a layered macromolecular structure with alternating amorphous and semicrystalline growth rings with a thickness of 120 to 400 nm and a semicrystalline ring formed by a cluster structure of alternating crystalline and amorphous regions with a 9 nm repeating distance [10]. Its special macromolecular structure makes it difficult to expose the enzymatic cleavage sites of starch. Therefore, traditional enzymatic hydrolysis has limitations in practical applications, such as low enzymatic hydrolysis efficiency, low amylose release, and low RS3 yield. To address these limitations, there is an urgent need to develop more effective ways for improving enzymolysis.

As a novel physical processing method, ultrasound has been extensively used in the research and application of food. Due to its unique cavitation, mechanical, and thermal effects, ultrasound can alter the structure, composition, and physicochemical properties of starch to a certain extent [11]. Power ultrasound could contribute to the depolymerization of retrograded starch, forming shorter chain molecules and reducing sugars, thereby increasing the water solubility of starch and reducing the viscosity of starch solutions [10]. Monroy et al. [11] found that ultrasound induced changes in morphological characteristics and crystallinity degrees of the cassava starch granules. Furthermore, the ultrasonic pretreatment was found to increase the enzyme's activity and encourage the mass transfer, thereby accelerating the enzyme-catalyzed reaction [12]. As a result, ultrasound treatment could change the structure of macromolecular substances and improve the efficiency of enzymolysis. Yet, the investigations on ultrasonic-assistedα-amylase hydrolysis to prepare RS3 are scanty.

Arrowhead is a perennial aquatic plant, widely distributed in Canada, the United States, China, and other parts of the world; dried arrowhead bulbs have been found to contain more than 50% starch making arrowhead a good source of starch [13]. Our previous research has successfully prepared resistant starch by enzymatic hydrolysis of its amylopectin by pullulanase using the arrowhead-derived starch as a raw material [14]. As an in-depth analysis of the composition of arrowhead starch, it was found to contain up to 50% amylose in addition to a large amount of amylopectin [13]; the molecular weight of its amylose was too high to escape directly from the starch, and the amylose with inappropriate molecular weight might be difficult to form RS3. Since amylose is a polysaccharide chain linked by D-glucosyl with a-(1, 4) glycosidic bond, α-amylase can well hydrolyze the α-1,4-glycosidic bond in amylose, amylopectin, and related oligosaccharides. As a result, this study was carried out to employ α-amylase to destroy macromolecular amylose and shorten the length of amylopectin to prepare RS3 as well as to include ultrasonic technology in the enzymatic hydrolysis process. Based on optimized ultrasonic conditions, the effects of ultrasonic treatment on the swelling power, water holding capacity, solubility, and transparency of arrowhead RS3 were studied. Besides, the effects of ultrasound on iodine absorption, thermal stability, relative crystallinity, and structural properties were also studied.

2. Materials and Methods

2.1. Materials. Arrowhead tubers within 24 hours of harvest were purchased from a vegetable market in Zheng Jiang, China, and its starch was immediately extracted using the method of Wang et al. [15]. Alpha-amylase (10000 U/g) was supplied by the Rui Yang Bio-Technology Co., Ltd (Su Zhou, China). The chemicals and reagents used in this study were of analytical grade.

2.2. Use of Ultrasound-Assisted Enzymolysis (UAE) to Prepare Arrowhead-Derived RS3. RS3 was prepared according to Simsek and El [3] with minor modifications. The arrowhead-derived starch (25 g, dry weight) was evenly dispersed in 200 mL of water and preheated in a 70°C water bath for 10 min. After cooling to 60°C, the pH of the starch slurry was brought to 6.0 using 0.05 M HCl and α-amylase (0.05 U/g starch) was added. The enzyme and starch mixture were incubated at 60°C for 20 min for enzymatic degradation. Based on the experimental design, the first partial enzymatic hydrolysis was carried out under an ultrasound field, and the other enzymolysis remained unchanged. Multimodel frequency power ultrasound equipment detailed in the previous research [16] was introduced to assist the enzymolysis reaction. The ultrasonic conditions were as follows: ultrasonic frequency, 20/35/50 kHz; time, 5, 10, 15, and 20 min; ultrasonic power density, 60, 120, 180, and 300 W/L; pulsed on-time/off-time, 5/5, 10/5, 15/5, 20/5, 25/5, and 30/5. A circulating hot water bath was used to keep the sample temperature at 60°C during sonication. Once the enzymatic hydrolysis was over, the blend was heated using boiling water to inactivate the enzyme for 10 min, and its pH was kept at 7. The samples were then incubated at 4°C for 24 h to recrystallize to form retrograded starch (RS3). The RS3 was filtered using a Whatman #1 filter paper and the precipitate after three washings was collected, lyophilized, ground, and stored. The RS3 prepared by traditional-enzymolysis and ultrasound-assisted enzymolysis (optimal ultrasound conditions) were named as RS3-E and RS3-UAE, respectively.

2.3. Determination of RS Yield. The yield of resistant starch was calculated using the official AOAC method no. 2002.02 as described in detail in previous studies [17].

2.4. Solubility and Swelling Power (SP). The starch samples were uniformly dispersed in water at a concentration of 2 g/100 mL and kept in the water bath at 80°C, 90°C, and 100°C for 30 min. The gelatinized starch samples were then centrifuged at 4500 ×g for 15 min. The supernatant and sediment were collected separately and measured.

The supernatant was concentrated and dried to a constant weight at 105°C, and the remaining precipitate was weighed directly. The solubility and SP were calculated as follows:

$$\text{Solubility}\,(S)\,(\%) = \frac{W_d}{W_t}\,\text{x}\,100,$$
$$SP\,\frac{g}{g} = \frac{W_s}{[W_t\,\text{x}\,(100\% - S)]}, \quad (1)$$

where W_d is the weight of the dried supernatant; W_t is the dry weight of the starch; and W_s is the weight of the starch sediment.

2.5. The Water Holding Capacity (WHC) and Transparency. The water holding capacity of the starch samples was analyzed by the method of Biswas et al. [18] with slight modification. Starch samples were dried in an oven at 105°C until a constant weight was achieved. Then, 0.5 g of the samples mixed with 6 mL of distilled water were added to a preweighed centrifuge tube. And then the tube was incubated in a water bath at 35°C for 1 h, and immediately centrifuged at 7500 g for 10 min. The supernatant was carefully removed and the precipitate was accurately weighed. The WHC was calculated as the ratio of the weight of the precipitate to the dry weight of the sample. The transparency of the samples was conducted following a reported approach with slight modification [19]. Incubation of the 1% starch suspension at 100°C for 20 minutes was conducted in a water bath. Upon cooling to room temperature, an ultraviolet/visible spectrophotometer (Beifen-Ruili Analytical Instrument Co., Ltd., Beijing, China) was used to measure the transparency at 620 nm.

2.6. Iodine Absorption. The iodine absorption capacity was determined using a spectrophotometer according to Qin et al. [20], and the scanning wavelength was from 500 nm to 800 nm.

2.7. Fourier-Transform Infrared (FT-IR) Spectroscopy. Two grams of dried starch samples were mixed with 300 mg of KBr and tableted under pressure. Sixteen scans were performed in the 4000–500 cm^{-1} range with a resolution of 4 cm^{-1} using an FTIR spectrophotometer (Thermo Electron Corporation, USA). The ratio of the absorbance values of the sample at wavelengths 1047 cm^{-1} and 1022 cm^{-1} was defined as 1047/1022 value.

2.8. X-Ray Diffraction (XRD). An X-ray diffractometer (XRD, D8 Advance, Bruker Inc., Germany) operated at voltage and current of 40 kV and 40 mA, respectively, was employed to record the X-ray diffraction pattern of starch samples. The following settings were scanning rate of 5°min^{-1} and Bragg angles (2θ) 5–30°. Starch samples were equilibrated in a desiccator containing saturated sodium chloride solution for 24 h prior to XRD analysis.

2.9. Thermal Properties. Thermal analysis of the starch samples was conducted using DSC (Q2000-DSC, New Castle, DE, USA) equipped with thermal analysis software [14]. Briefly, a 3 mg starch sample was accurately weighed into an aluminum pan and an appropriate amount of distilled water was added in a 1 : 3 (starch/water) ratio. The thermodynamic parameters gelatinization transition temperatures (starting temperature, T_o; the peak temperature, T_p; and the ending temperature, T_c), the gelatinization temperature range ($T_c - T_o$), and gelatinization enthalpy (ΔH) were calculated, respectively.

2.10. Morphology. A scanning electron microscope (SEM) Hitachi S-4800 (Hitachi High-Technologies, Tokyo, Japan) was used to observe the starch samples' morphology at an accelerating voltage of 1.0 kV. The samples were uniformly distributed on an aluminum plate with a two-sided adhesive tape for microscopic observation. Then, the samples were sprayed with gold under a vacuum. The SEM images were recorded at magnifications of 500x and 5000x, respectively.

2.11. Statistical Analysis. The results of all experiments were expressed in terms of mean +standard deviation, and the experiments were conducted at least in triplicate. The data were analyzed by analysis of variance (ANOVA) and the Tukey test at a 95% confidence level using SPASS version 17.0 software (SPSS Inc., Chicago, Illinois, USA).

3. Results

3.1. Arrowhead-Derived Resistant Starch Yield. The resistant starch yields of native arrowhead starch, RS3-E, and RS3-UAE are presented in Figure 1. It could be seen that the resistant starch content of the native starch was 5.36%. After the arrowhead-derived starch was degraded by α-amylase, the content of the prepared resistant starch reached 10.39%. Ultrasound treatment encouraged the enzymatic hydrolysis and altered the yield of resistant starch in RS3 to varying degrees. As shown in Figure 1(a), the resistant starch yield increased with increasing ultrasound power and reached its maximum value of 16.15% at 120 W/L. However, the resistant starch yield decreased when the ultrasound power was further increased, and this was similar to the results presented by Wang et al. [12]. The ultrasound power was closely related to the energy generated and transmitted by ultrasound. Ultrasound at certain intensity might negatively affect α-amylase to denature the enzyme and reduce its stability by disrupting the intermolecular interactions within the polypeptide chain. Figure 1(b) shows the effects of ultrasound time on the resistant starch yield. The results indicated that the highest resistant starch yield (15.31%) was obtained in response to 15 min ultrasound treatment, which was increased by 47.35% compared to that without ultrasound. However, the resistant starch yield gradually decreased as ultrasound time was increased, indicating that ultrasound treatment over a longer time period (>15 min) suppressed the production of RS. The promotion effects of resistant starch obtained by 20 min ultrasound treatments are still remarkable, as demonstrated herein. By improving enzymatic reaction rates, ultrasound treatment could also decrease activation energy, enthalpy, Gibbs free energy, and

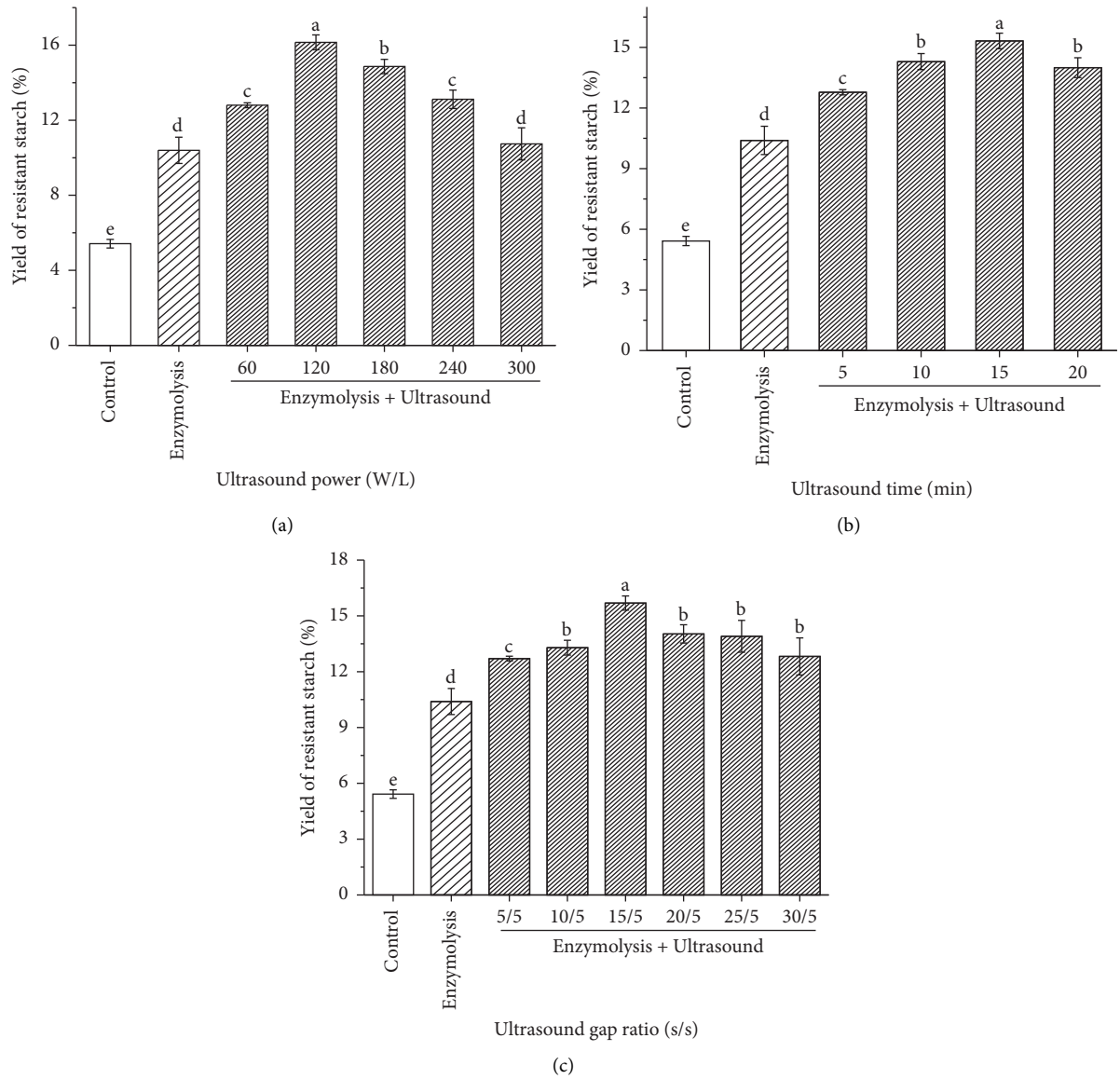

Figure 1: Effects of ultrasound treatment using different powers (a), times (b), pulsed on-time/off-time parameter (c) on resistant starch yield. Different letters indicate significant differences ($p < 0.05$).

entropy of activation, thereby increasing enzymolysis efficiency [21]. As can be seen from the results in Figure 1(c), the resistant starch yield reached its highest (15.68%) under ultrasound treatment operating with a pulsed on-time/off-time of 15 s/5 s. This appropriate intermittent ultrasound can successfully disrupt the structure of the starch clusters, and decompose starch chains, thereby reducing starch's molecular weight. Furthermore, the starch fragments isolated from the interwoven clusters increased the contact sites to α-amylase, which eventually improved the enzymatic hydrolysis effect and promoted the production of amylose and amylopectin with a suitable degree of polymerization, resulting in an increase in resistant starch production.

According to the above single-factor experiment results, the ultrasound treatment conditions were as follows: ultrasonic power density, 120 W/L; time, 15 min; and ultrasound intermittent ratio, 15 s/5 s. Under the above ultrasonic conditions, the resistant starch yield reached 17.21% (Table 1). Compared with traditional enzymatic degradation, the yield of resistant starch significantly ($p < 0.05$) increased by 65.64%. Furthermore, the RS3-UAE prepared by the optimal ultrasonic conditions-assisted enzymatic hydrolysis combined with the retrogradation in the later stage was used for the later physicochemical properties and structural analysis.

3.2. Functional Properties. Functional properties such as solubility, swelling power, transparency, and WHC were dependent on the size, granule morphology, amylose content, and molecular structure of starch, summarized in Table 1. The solubility of starch is the percentage of starch granules dissolved at a certain temperature; the mass proportion of water absorbed per gram of dried starch at

Table 1: Changes in swelling power, water holding capacity, solubility, and transparency. RS3-E type 3 resistant starch prepared by traditional-enzymolysis; RS3-UAE type 3 resistant starch prepared by ultrasound-assisted enzymolysis.

	Native arrowhead starch	RS-E	RS-UAE
Resistant starch yield (%)	5.36 ± 0.21^{c}	10.39 ± 0.53^{b}	17.21 ± 0.55^{a}
Solubility (%)			
70°C	2.83 ± 0.44^{c}	40.21 ± 1.2^{a}	40.47 ± 1.32^{a}
80°C	3.25 ± 0.12^{c}	40.34 ± 1.11^{b}	45.72 ± 1.16^{a}
90°C	3.53 ± 0.17^{b}	41.60 ± 0.76^{b}	47.49 ± 0.54^{a}
Swelling power (g/g)			
70°C	16.1 ± 0.12^{a}	6.42 ± 0.11^{c}	7.51 ± 0.12^{b}
80°C	15.65 ± 0.21^{a}	8.37 ± 0.17^{b}	6.72 ± 0.15^{c}
90°C	14.79 ± 0.30^{a}	7.36 ± 0.16^{b}	6.33 ± 0.14^{b}
Transparency (%)	6.35 ± 0.86^{c}	27.6 ± 2.34^{a}	20.45 ± 2.09^{b}
Water holding capacity (%)	254.23 ± 15.11^{c}	367 ± 20.32^{b}	423 ± 30.16^{a}

*different letters indicate significant differences ($p < 0.05$).

a certain temperature is known as swelling power. It was observed that the solubility and SP of samples increased with the rise in temperature (70°C–90°C), indicating that temperature could directly affect the solubility and SP. As the temperature increased, the interaction between starch molecules might be reduced, resulting in swollen, loose, or even collapsed structure of starch; when it encountered water, short amylose escaped from the starch granules. Also, the water molecules penetrated into the RS3 and interacted with the starch molecules through hydrogen bonds, resulting in the gradual increase of solubility and swelling power, and the formation of gelatinization. These results were consistent with Kudzu (*Pueraria lobata*)-derived resistant starch prepared by debranching and subsequent recrystallization using cyclic temperature and isothermal conditions [19]. Moreover, the solubility of RS3 was significantly higher than that of pure starch at the same temperature, while the swelling power had the opposite effect. Similar results were reported by Liang et al. [16], who reported similar trends for these two indicators after enzymatic debranching. Enzymatic hydrolysis destroyed the crystal structure of natural starch; the intermolecular force in RS3 formed by amylose obtained by enzymatic hydrolysis was weakened, which easily led to the redissolution of amylose. It could be further speculated that the escape of a large amount of amylose from the RS3 led to a decrease in dry matter and swelling ability. The solubility of RS3-E at 80°C and 90°C was significantly ($p < 0.05$) lower than that of RS3-UAE, and its swelling power was significantly higher ($p < 0.05$) compared to RS3-UAE, providing that the method of ultrasonic-assisted enzymatic hydrolysis can increase the solubility of the prepared resistant starch and decrease its swelling ability. The reason might be attributed to ultrasound-assisted enzymatic hydrolysis, which reduced the yield of amylopectin and produced more amylose with good solubility, resulting in poor swelling power [18]. Chang et al. [22] also found that ultrasound mainly attacked the amorphous regions of granules and amylose, which was easier than highly branched amylopectin; ultrasound can degrade starch chains into very short chains and further cut long starch chains into appropriate lengths. In addition, the difference in chain cleavage (glycosidic bond cleavage) during enzymolysis may also cause an increase in molecular polarity and a decrease in interchain hydrogen bonds, which also could explain the increase in solubility. In addition, the surface of RS3-UAE particles obtained after ultrasonic treatment tends to be smooth and flat, and there is no fragmentation and voids (Figure 2), which was not conducive to water diffusion, resulting in a decrease in its swelling capacity.

The transparency of starch samples reflects the optical changes in starch after gelatinization. The transparency is closely related to the swelling capacity, number of unexpanded granules, and amylose content. Recent studies have also found that the smaller the starch granules, the less likely they will swell with water and reflect and refract light, making starch samples more transparent [23]. The order of transparency is RS3-UAE > RS3-E > native starch (Table 1), indicating that the enzymolysis degradation and retrogradation process could improve the transparency of native starch. Furthermore, ultrasound treatment could remarkably increase the light transmittance, resulting in improved transparency of RS3.

WHC provides information about the starch's ability to retain water under gravity, which is linked to the structure and physicochemical properties of starch granules. Compared with untreated starch, the WHC of RS3 was significantly increased (Table 1). The above results might be attributed to the increased proportion of short-chain amylose in RS3 compared to native starch, and the hydrophilic hydroxyl groups outside the glucose unit increased the chance of ordered arrangement and coalescence [19]. The WHC value of RS3-UAE was significantly ($p < 0.05$) higher than that of RS3-E, representing that ultrasound-assisted enzymatic degradation enhanced the WHC of RS3. It has been reported that both the amylose content and amylose chain length could affect the values of WHC; the neat and long linear short starch chains had more opportunities to align and aggregate, leading to chain aggregation and the formation of gel network formation through hydrogen bonding and hydrophobic interactions [24]. Therefore, it could be speculated that the amylose composition in RS3-UAE was different from that in RS3-E; ultrasonic-assistedα-amylase degradation might increase the content of long amylose and make the amylose produced by enzymolysis more uniform.

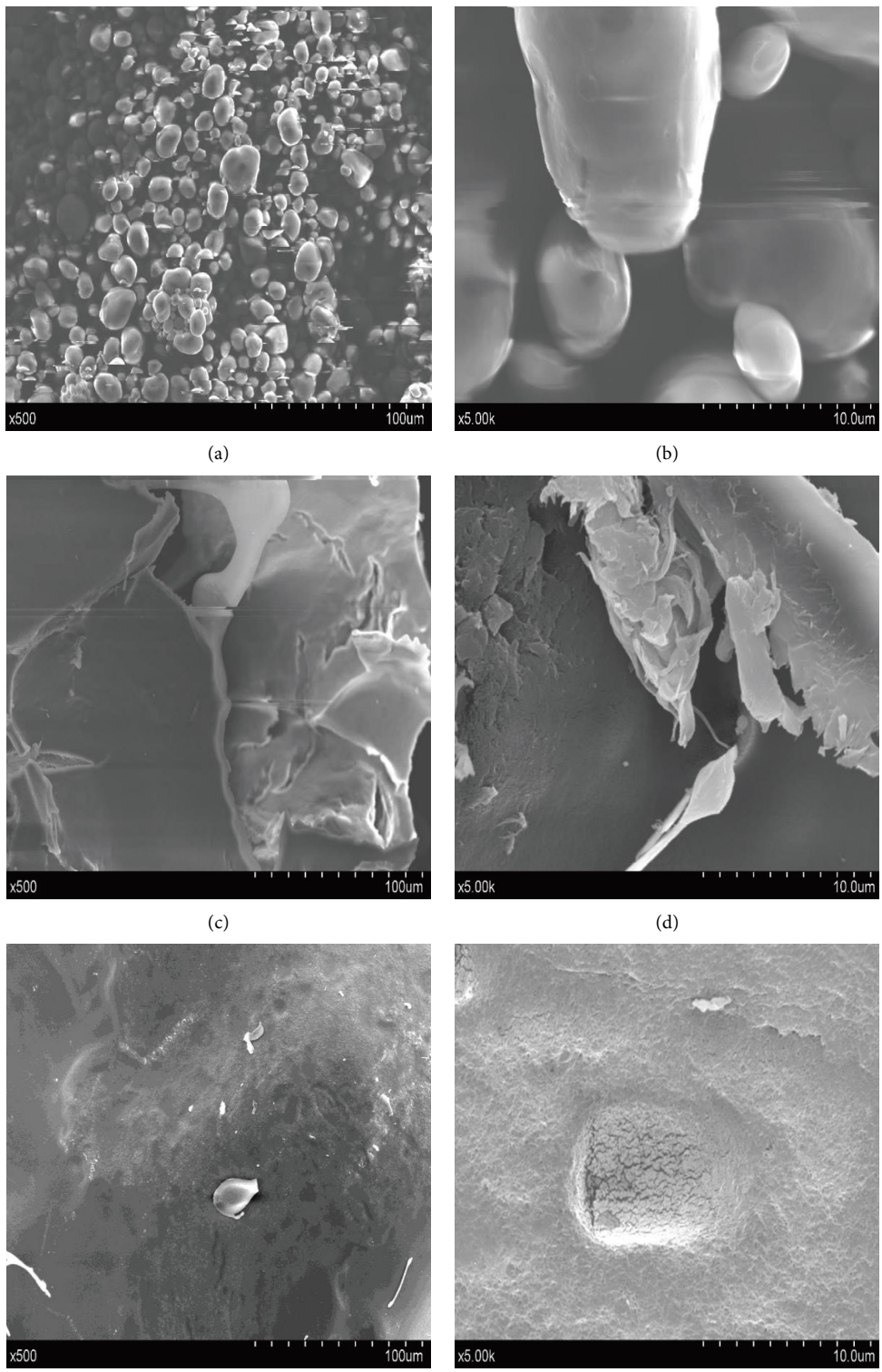

(a) (b)

(c) (d)

(e) (f)

Figure 2: Morphological changes in arrowhead starch (a), (b), RS3-E (c), (d), RS3-UAE (e), and (f) (magnification: 500x and 5000x). RS3-E type 3 resistant starch prepared by traditional-enzymolysis; RS3-UAE type 3 resistant starch prepared by ultrasound-assisted enzymolysis.

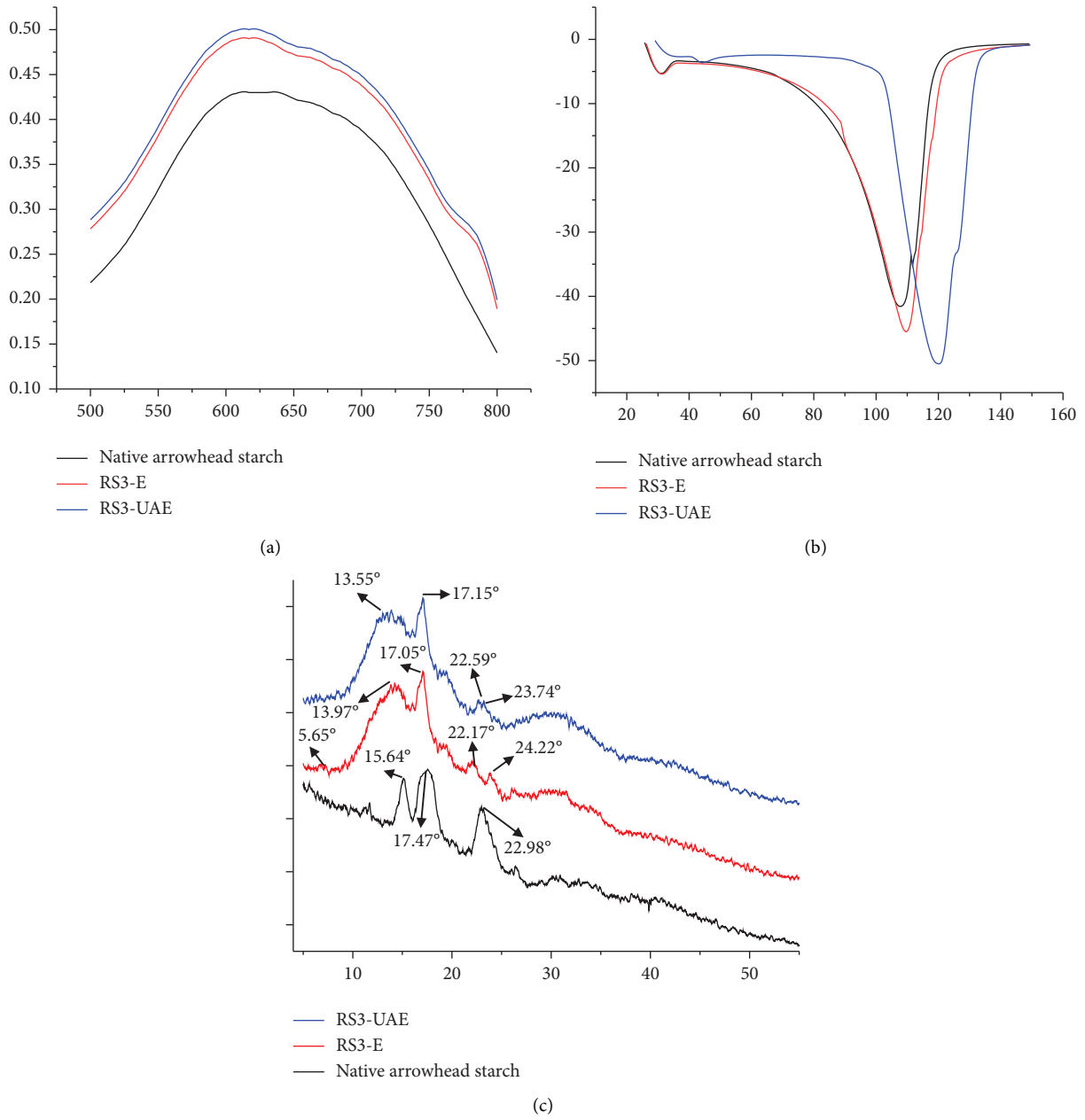

Figure 3: The iodine absorption curve (a), DSC thermograms (b), and XRD diffractograms (c) of arrowhead starch, RS3-E, and RS3-UAE. RS3-E type 3 resistant starch prepared by traditional-enzymolysis; RS3-UAE type 3 resistant starch prepared by ultrasound-assisted enzymolysis.

3.3. Iodine Absorption. The iodine absorption curves of starch samples with wavelengths from 450 to 800 nm were recorded and shown in Figure 3(a). It is known that the combination of amylose and iodine produces a spiral complex, which has a maximum absorption peak in the wavelength of 600–640 nm; while the long chain of amylopectin forms a complex with iodine, which has the maximum absorption peak in 520–560 nm [20]. As shown in Figure 3, all starch samples had absorption intensity between 520–720 nm and the most prominent absorption peak appeared at 600–650 nm. Since native starch contained part of amylopectin, it was theoretically speculated that native starch should have an absorption peak at 520–560 nm, which was contrary to the experimental results. The reason might be that the interaction between amylopectin and iodine was weak [25]. Its maximum absorption peak might be covered by the absorption peak of the complex formed by amylose and iodine, and thus it could not be observed. Based on the intensity of the absorption peak, the absorption capacity of iodine in the starch samples could be sorted as follows: RS3-UAE > RS3-E > native starch. The absorbance measured by spectrophotometry and the maximum absorbance wavelength were decided by the degree of polymerization and the structural properties of the starch molecule [26]. The above

results showed that compared with traditional enzymatic hydrolysis, ultrasonic-assisted enzymatic hydrolysis changed the structure and composition of RS3 and increased the starch content with the same degree of polymerization. Furthermore, it could be inferred that the amylose content of RS3-UAE prepared by ultrasonic-assisted enzymatic degradation might be higher than that of traditional enzymatic degradation.

3.4. DSC. The DSC curves of the starch samples and their corresponding thermal parameters are shown in Figure 3(b) and Table 2, respectively. The transition temperatures of starch samples are in ascending order, RS3-UAE < RS3-E < native starch. Compared with natural starch, RS3 showed a higher DSC transition temperature. The results indicated that the RS3-UAE had a more ordered crystal structure and higher crystallinity than RS3-E. Furthermore, the starch's crystallinity and gelatinization temperature are positively correlated with its chain length and amylose content [18]. Therefore, from the higher crystallinity of RS3-UAE, it could be further speculated that ultrasonic-assisted enzymatic hydrolysis might obtain more amylose with suitable chains length. The gelatinization temperature range (T_c-T_o) of starch samples could reflect the uniformity and stability; an increase in the T_c-T_o value indicated the crystal regions with various crystallites in starch granules [27]. The native starch showed the lowest value of $T_c - T_o$, and the RS3-UAE had the highest value, suggesting that the native starch had the highest homogeneity and stability in the crystalline domains. From another perspective, various starch chains produced by the degradation of α-amylase were retrograded and formed a starch particle with more crystallites in the crystal domains compared to the native starch, and ultrasound aggravated this phenomenon. Enthalpy (ΔH) is mainly influenced by the disappearance of the double helix structure in the crystalline region; the higher the ΔH, the more energy is required for the dissociation of the double helices [28]. RS3-UAE possessed the highest ΔH value compared with native arrowhead starch. The rise in ΔH value of RS3-UAE could be speculated to the increased intermolecular forces during the annealing process. In addition, compared with traditional enzymatic degradation, the ultrasound modified the structure and chain length of amylose, which might help to improve RS3-UAE's order and stability of the double helix.

3.5. Changes in Diffractograms. Figure 3(c) presents the XRD spectra of the native starch and RS3, and its corresponding relative crystallinity is summarized in Table 2. Crystalline type of the starch is currently divided into A, B, and C types according to the peak at different diffraction angles on the XRD spectrum [3]. The starch derived from arrowhead corm showed a typical A-type crystalline structure, with peaks at 15°, 17°, 18°, and 23°, which was in agreement with previous results [29]. However, the prepared RS3 was found to have a B-type crystalline pattern, with a strong peak at 17°, several small peaks near 15°, 20°, 22°, and 24°, and an additional peak near 5.6°. This result indicated that the RS3 obtained by the combination of α-amylase degradation and retrogradation showed a different crystalline type than its native starch. Similarly, the crystal form of the resistant starch prepared by ultrasonic-assisted pullulanase enzymatic hydrolysis was changed from native starch type A to type B [14]. Obviously, the XRD patterns of RS3-E and RS3-UAE were different, even though they were both B-type crystals, which could be due to the different preparation methods. After calculation, it was found that the relative crystallinity of RS3-UAE (38.44%) was significantly higher than that of RS3-E (35.71%). In fact, the crystal structure and relative crystallinity of starch depend on the amylose double helix, the degree of intermolecular association, amylopectin chain length and crystal size [18]. During α-amylase enzymolysis reactions, the sufficient combination of enzymes and substrates induced by ultrasound would speed up the reaction and increase the content of amylose produced, which provided new opportunities for arrangement and aggregation to form a compact double helix structure, thereby increasing the relative crystallinity of RS3-UAE.

3.6. FTIR Spectra. The FT-IR spectrum presents the characteristic bands of the main functional groups of starch corresponding to stretching, buckling, and deformation; the FT-IR spectra provide information about the changes in the molecular structure of starch samples. The spectral changes in the samples are present in Figure 4. All samples showed similar peaks at 927.42 cm^{-1}, 1081.28 cm^{-1}, 1154.89 cm^{-1}, 1647.94 cm^{-1}, 2930.64 cm^{-1}, and 3100–3700 cm^{-1}, which represented asymmetric stretching vibrations of D-pyranoglucose, C-O stretching vibrations of glycosidic bonds, some C-OH stretching vibrations of C-O, $-CH_2OH$ ring bending vibrations of glucose, intramolecular absorption peaks of hydrogen bonds, C=O stretching vibrations of aldehyde groups, C-H stretching vibrations and the stretching vibration of –OH, respectively [27]. The above results indicated that neither new chemical groups were generated nor the types of chemical groups in starch molecules were changed during the preparation of RS3-E and RS3-UAE. In addition, the peak at 2930.64 cm^{-1} representing the stretching vibration of $-CH_2$ in polysaccharides showed the hydrophobicity of starch to some extent [30]. The decrease in the methylene peak of RS3-UAE showed an improvement in starch's hydrophilicity, which might also lead to an increase in its solubility and water holding capacity (Table 1). It was carefully observed and found that although the peak positions of the three starch samples were the same, the shape and intensity of the peaks appeared different. It suggested that both α-amylase enzymolysis and ultrasound-assistedα-amylase enzymolysis altered the crystallinity and conformation of the starch molecules. In particular, the IR ratios at 1047/1022 cm^{-1} could be used as an intensity indicator of crystalline and amorphous regions; the higher values of $R_{1047/1022}$ reflect more crystalline regions [27]. The 1047/1022 ratio values of the starch samples were decreased in the following order, RS3-UAE > nativestarch > RS3-E, which was in correspondence with the crystallinity results in Table 2. The increased

Table 2: Effects of ultrasound-assisted enzymolysis on thermal parameters, relative crystallinity (RC %), and the ratio of 1047/1022 cm^{-1} for native arrowhead starch, RS3-E, and RS3-UAE. RS3-E type 3 resistant starch prepared by traditional-enzymolysis; RS3-UAE type 3 resistant starch prepared by ultrasound-assisted enzymolysis.

Sample	T_O (°C)	T_p (°C)	T_C (°C)	$T_C - T_O$ (°C)	ΔH (J/g)	RC (%)	1047/1022
Native arrowhead starch	87.8 ± 0.14^c	107.8 ± 0.78^c	110.7 ± 0.54^c	22.9 ± 0.34^b	8.2 ± 0.29^a	36.76 ± 0.88^b	0.876 ± 0.001^b
RS3-E	88.8 ± 0.55^b	109.5 ± 0.30^b	113.1 ± 0.34^b	23.3 ± 0.43^b	9.5 ± 0.78^b	35.71 ± 0.84^b	0.831 ± 0.002^c
RS3-UAE	102.1 ± 1.11^a	120.1 ± 0.66^a	133.3 ± 0.98^a	31.2 ± 0.85^a	12.3 ± 0.90^a	38.44 ± 1.13^a	0.886 ± 0.004^a

*different letters indicate significant differences among different groups ($p < 0.05$).

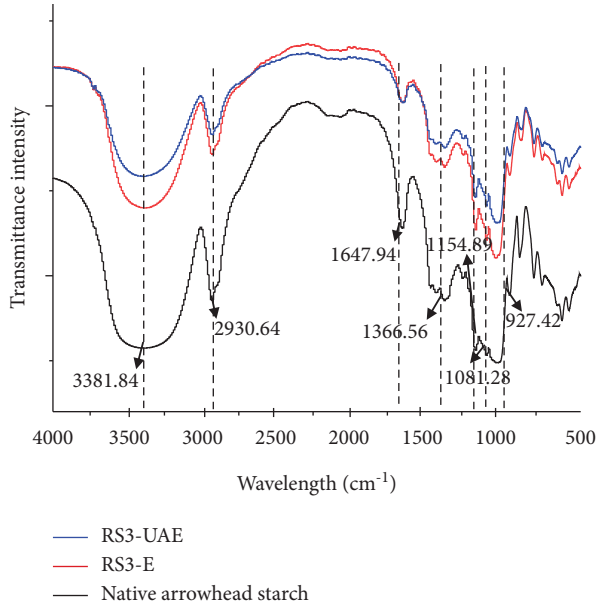

Figure 4: FTIR spectral changes in native arrowhead starch, RS3-E, and RS3-UAE. RS3-E type 3 resistant starch prepared by traditional-enzymolysis; RS3-UAE type 3 resistant starch prepared by ultrasound-assisted enzymolysis.

crystallinity of RS3-UAE also indirectly reflected that ultrasound-assistedα-amylase degradation significantly improved the relatively ordered structures of RS3 compared with RS3-E [14].

3.7. SEM. The morphological changes in the samples were observed by scanning electron microscopy, and its SEM micrographs magnified 500 times and 5000 times were shown in Figure 2. The starch derived from the arrow was oval in shape, smooth in surface, uniform in size, and about 5–10 μm in diameter, indicating that the starch granules were intact and not attacked by enzymes and chemical reagents. The shape of arrowhead-derived starch granules was different from grains such as rice, wheat, and corn, but similar to tubers, such as potatoes. Furthermore, Li et al. [29] studied the morphology of different arrowhead starches (Purple-corm, Hongta, and Japanese arrowhead) and found its average granule sizes were 5.36, 9.82, and 9.06 μm, respectively; these results were consistent with the current research results. Compared to native starch, a remarkably visible difference in granule shape was observed for RS3; the molecular weight of RS3 was so large that the possible particle structure of RS3 could not be seen at 500 magnifications. The particle size seemed to be larger than 100 μm. From Figures 2(c) and 2(d), it could be seen that the surface of RS3-E particles had layered strips and folds. The above phenomenon was attributed to the α-amylase degradation of starch granules combined with recrystallization [18]; the native starch was enzymatically hydrolyzed to a large amount of short-chain amylose, which was rearranged and aggregated at low temperature, thus forming RS3 with characteristic lumps and irregularities. Zeng et al. [19] also reported similar research results that the kudzu (*Pueraria lobata*) derived-starch structure was destroyed after enzymolysis, gelatinization, and retrogradation, and the formed resistant starch showed rough irregular shapes of different sizes. Unsurprisingly, RS3-UAE particles had a different morphology than RS3-E, with RS3-UAE particles having a smoother surface and a denser structure. It was due to the sonication applied during enzymatic degradation prior to retrogradation. Ultrasound could change the structure of starch to a certain extent, affecting its physicochemical, rheological, morphological, and functional properties [12]. Furthermore, ultrasound, at certain level of intensity, could cause the intermolecular forces and structural changes of the protein, resulting in the activation of α-amylase [31]. Additionally, when ultrasound propagated in the medium, strong acoustic currents, microjets, and shock waves were generated in the liquid medium, which reduced the diffusion

limiting barrier around the reactants, enhanced heat, and mass transfer, and promoted the enzyme-substrate binding rates in the reaction system [32].

4. Conclusions

The arrowhead-derived resistant starch type-3 was successfully prepared by the α-amylase enzymolysis method and the ultrasound-assisted α-amylase enzymolysis method. Its resistant starch contents were greatly increased compared with the resistant starch in the native arrowhead. The arrowhead-derived RS3 prepared exhibited a typical B crystal structure, and it possessed a large particle size, with layered strips and a wrinkled surface. Compared to RS3-E, RS3-UAE exhibited different functional properties, higher solubility, WHC, lower transparency, and higher swelling power at 70°C. Additionally, RS3-UAE showed a more regular shape, a smoother surface, a higher crystallinity, a stable double helix structure, and a more ordered and denser structure according to iodine absorption, DSC, XRD, FTIR, and SEM analyses. The above results provide good theoretical support for applying ultrasound in the preparation of RS3 by enzymatic hydrolysis. As the physiochemical and structural properties of RS3 were closely related to the preparation method, which might affect the physiological functions of RS3. Therefore, further animal or cell experiments are still needed to understand the bioavailability and in vivo efficacy of RS3-UAE.

Data Availability

Data are available upon request.

Conflicts of Interest

The authors declare that they have no conflicts of interest.

Authors' Contributions

Conceptualization was performed by Xiaofeng Ren. Methodology was performed by Qiufang Liang. Experiment operation was performed by Liangge Sun and Xinxiang Chen. Software was used by Jian Sun. Validation was performed by Gangshan Wu and Xiaofeng Ren. Writing of original draft, preparation, and review and editing was performed by Jian Sun and Qiufang Liang. Funding Acquisition was performed by Jian Sun.

Acknowledgments

The authors would like to express their appreciation for the support obtained from the Jiangsu Agricultural Science and Technology Innovation Fund (Grants no. CX (20) 3044), The Primary Research & Development Plan of Zhenjiang (Grants no. NY2020011), Key Laboratory of Modern Agricultural Equipment and Technology (Jiangsu University), the Youth Support Project of Jiangsu Vocational College of Agriculture and Forestry (no. 2020kj013), and the Special Project for Scientific Research Institutes of Zhejiang Province (no. 2021YSZX007).

References

[1] A. A. Alsaffar, "Effect of food processing on the resistant starch content of cereals and cereal products - a review," *International Journal of Food Science and Technology*, vol. 46, no. 3, pp. 455–462, 2011.

[2] S. Ma, Z. Wang, H. Liu et al., "Supplementation of wheat flour products with wheat bran dietary fiber: purpose, mechanisms, and challenges," *Trends in Food Science & Technology*, vol. 123, pp. 281–289, 2022.

[3] S. Simsek and S. N. El, "Production of resistant starch from taro (Colocasia esculenta L. Schott) corm and determination of its effects on health by in vitro methods," *Carbohydrate Polymers*, vol. 90, no. 3, pp. 1204–1209, 2012.

[4] M. Shi, Y. Chen, S. Yu, and Q. Gao, "Preparation and properties of RS III from waxy maize starch with pullulanase," *Food Hydrocolloids*, vol. 33, no. 1, pp. 19–25, 2013.

[5] S. Ozturk, H. Koksel, K. Kahraman, and P. K. W. Ng, "Effect of debranching and heat treatments on formation and functional properties of resistant starch from high-amylose corn starches," *European Food Research and Technology*, vol. 229, no. 1, pp. 115–125, 2009.

[6] L. Wang, Q. Wang, J. Qian et al., "Bioavailability and bioavailable forms of collagen after oral administration to rats," *Journal of Agricultural and Food Chemistry*, vol. 63, no. 14, pp. 3752–3756, 2015.

[7] H. Zhang and Z. Jin, "Preparation of products rich in resistant starch from maize starch by an enzymatic method," *Carbohydrate Polymers*, vol. 86, no. 4, pp. 1610–1614, 2011.

[8] C. W. Simons, C. Hall, and S. Vatansever, "Production of resistant starch (RS3) from edible bean starches," *Journal of Food Processing and Preservation*, vol. 42, no. 11, Article ID e13587, 2018.

[9] F. J. Warren, B. Zhang, G. Waltzer, M. J. Gidley, and S. Dhital, "The interplay of alpha-amylase and amyloglucosidase activities on the digestion of starch in in vitro enzymic systems," *Carbohydrate Polymers*, vol. 117, pp. 192–200, 2015.

[10] J. Zhu, L. Li, L. Chen, and X. Li, "Study on supramolecular structural changes of ultrasonic treated potato starch granules," *Food Hydrocolloids*, vol. 29, no. 1, pp. 116–122, 2012.

[11] Y. Monroy, S. Rivero, and M. A. García, "Microstructural and techno-functional properties of cassava starch modified by ultrasound," *Ultrasonics Sonochemistry*, vol. 42, pp. 795–804, 2018.

[12] D. Wang, F. Hou, X. Ma et al., "Study on the mechanism of ultrasound-accelerated enzymatic hydrolysis of starch: analysis of ultrasound effect on different objects," *International Journal of Biological Macromolecules*, vol. 148, pp. 493–500, 2020a.

[13] S. M. Chang, "Characterization of starch from sagittaria trifolia L. Var. Sinensis makino," *Journal of Food Science*, vol. 53, no. 3, pp. 837–840, 2010.

[14] Q. Liang, X. Chen, X. Ren, X. Yang, H. Raza, and H. Ma, "Effects of ultrasound-assisted enzymolysis on the physicochemical properties and structure of arrowhead-derived resistant starch," *Lebensmittel-Wissenschaft & Technologie*, vol. 147, Article ID 111616, 2021.

[15] B. Wang, T. Meng, H. Ma et al., "Mechanism study of dual-frequency ultrasound assisted enzymolysis on rapeseed protein by immobilized Alcalase," *Ultrasound Sonochemisty*, vol. 32, pp. 307–313, 2016.

[16] Q. Liang, X. Ren, X. Zhang et al., "Effect of ultrasound on the preparation of resveratrol-loaded zein particles," *Journal of Food Engineering*, vol. 221, pp. 88–94, 2018.

[17] X. Hui, Z. Zhi, L. Jie, T. Xiang, and L. Wen, *Study on Resistant Starch Determination Methods*, Journal of Henan University of Technology (Natural ence Edition, Henan, China, 2012.
[18] P. Biswas, M. Das, S. Boral, G. Mukherjee, K. Chaudhury, and R. Banerjee, "Enzyme mediated resistant starch production from Indian Fox Nut (Euryale ferox) and studies on digestibility and functional properties," *Carbohydrate Polymers*, vol. 237, 2020.
[19] F. Zeng, T. Li, H. Zhao, H. Chen, X. Yu, and B. Liu, "Effect of debranching and temperature-cycled crystallization on the physicochemical properties of kudzu (Pueraria lobata) resistant starch," *International Journal of Biological Macromolecules*, vol. 129, pp. 1148–1154, 2019.
[20] W. Qin, C. Wen, J. Zhang et al., "Structural characterization and physicochemical properties of arrowhead resistant starch prepared by different methods," *International Journal of Biological Macromolecules*, vol. 157, pp. 96–105, 2020.
[21] W. Qu, H. Ma, B. Liu, R. He, Z. Pan, and E. E. Abano, "Enzymolysis reaction kinetics and thermodynamics of defatted wheat germ protein with ultrasonic pretreatment," *Ultrasonics Sonochemistry*, vol. 20, no. 6, pp. 1408–1413, 2013.
[22] R. Chang, H. Lu, X. Bian, Y. Tian, and Z. Jin, "Ultrasound assisted annealing production of resistant starches type 3 from fractionated debranched starch: structural characterization and in-vitro digestibility," *Food Hydrocolloids*, vol. 110, Article ID 106141, 2021.
[23] A. Hu, L. Li, J. Zheng et al., "Different-frequency ultrasonic effects on properties and structure of corn starch," *Journal of the Science of Food and Agriculture*, vol. 94, no. 14, pp. 2929–2934, 2015.
[24] H. S. Guraya, C. James, and E. T. Champagne, "Effect of enzyme concentration and storage temperature on the formation of slowly digestible starch from cooked debranched rice starch," *Starch - Stärke*, vol. 53, no. 3-4, pp. 131–139, 2015.
[25] E. Apostolidis and I. Mandala, "Modification of resistant starch nanoparticles using high-pressure homogenization treatment," *Food Hydrocolloids*, vol. 103, p. 7, 2020.
[26] D. Sievert and Y. Pomeranz, *Enzyme-resistant Starch. I. Characterization and Evaluation by Enzymatic, Thermoanalytical, and Microscopic Methods*, American Association of Cereal Chemists, Eagan, Minnesota, 1989.
[27] J. Zou, M. Xu, L. Wen, and B. Yang, "Structure and physicochemical properties of native starch and resistant starch in Chinese yam (Dioscorea opposita Thunb.)," *Carbohydrate Polymers*, vol. 237, 2020.
[28] Z. Guo, S. Zeng, X. Lu, M. Zhou, M. Zheng, and B. Zheng, "Structural and physicochemical properties of lotus seed starch treated with ultra-high pressure," *Food Chemistry*, vol. 186, pp. 223–230, 2015.
[29] A. Li, Y. Zhang, Y. Zhang et al., "Comparison of morphology and physicochemical properties of starch among 3 arrowhead varieties," *Journal of Food Science*, vol. 81, no. 5, Article ID C1110, 2016.
[30] X. Wang, X. P. Hu, Z. Wang et al., "Preparation and characterization of highly lipophilic modified potato starch by ultrasound and freeze-thaw treatments," *Ultrasonics Sonochemistry*, vol. 64, p. 7, 2020.
[31] H. Meng, D. Li, and C. Zhu, "The effect of ultrasound on the properties and conformation of glucoamylase," *International Journal of Biological Macromolecules*, vol. 113, 2018.
[32] J. Jin, H. B. Lin, A. A. Yagoub, S. L. Xiong, L. Xu, and C. C. Udenigwe, "Effects of high power ultrasound on the enzymolysis and structures of sweet potato starch," *Journal of the Science of Food and Agriculture*, vol. 100, no. 8, pp. 3498–3506, 2020.